Observational Study

Medicine®

OPEN

Correlation of iodine uptake and perfusion parameters between dual-energy CT imaging and first-pass dual-input perfusion CT in lung cancer

Xiaoliang Chen, MD, Yanyan Xu, MD, Jianghui Duan, MD, Chuandong Li, BS, Hongliang Sun, MD*, Wu Wang, MD, PhD

Abstract

To investigate the potential relationship between perfusion parameters from first-pass dual-input perfusion computed tomography (DI-PCT) and iodine uptake levels estimated from dual-energy CT (DE-CT).

The pre-experimental part of this study included a dynamic DE-CT protocol in 15 patients to evaluate peak arterial enhancement of lung cancer based on time-attenuation curves, and the scan time of DE-CT was determined. In the prospective part of the study, 28 lung cancer patients underwent whole-volume perfusion CT and single-source DE-CT using 320-row CT. Pulmonary flow (PF, mL/min/100 mL), aortic flow (AF, mL/min/100 mL), and a perfusion index (PI = PF/[PF + AF]) were automatically generated by in-house commercial software using the dual-input maximum slope method for DI-PCT. For the dual-energy CT data, iodine uptake was estimated by the difference (λ) and the slope (λHU). λ was defined as the difference of CT values between 40 and 70 KeV monochromatic images in lung lesions. λHU was calculated by the following equation: $\lambda HU = |\lambda/(70-40)|$. The DI-PCT and DE-CT parameters were analyzed by Pearson/Spearman correlation analysis, respectively.

All subjects were pathologically proved as lung cancer patients (including 16 squamous cell carcinoma, 8 adenocarcinoma, and 4 small cell lung cancer) by surgery or CT-guided biopsy. Interobserver reproducibility in DI-PCT (PF, AF, PI) and DE-CT (λ, λHU) were relatively good to excellent (intraclass correlation coefficient $[ICC]_{Inter} = 0.8726–0.9255$, $ICC_{Inter} = 0.8179–0.8842$; $ICC_{Inter} = 0.8881–0.9177$, $ICC_{Inter} = 0.9820–0.9970$, $ICC_{Inter} = 0.9780–0.9971$, respectively). Correlation coefficient between λ and AF, and PF were as follows: 0.589 ($P < .01$) and 0.383 ($P < .05$). Correlation coefficient between λHU and AF, and PF were as follows: 0.564 ($P < .01$) and 0.388 ($P < .05$).

Both the single-source DE-CT and dual-input CT perfusion analysis method can be applied to assess blood supply of lung cancer patients. Preliminary results demonstrated that the iodine uptake relevant parameters derived from DE-CT significantly correlated with perfusion parameters derived from DI-PCT.

Abbreviations: AF = aortic flow, DE-CT = dual-energy computed tomography, DI-PCT = dual-input perfusion computed tomography, DLP = dose-length product, ICC = intraclass correlation coefficient, PF = pulmonary flow, PI = perfusion index, ROI = region of interest, TDC = time-density curve.

Keywords: computed tomography, dual-energy CT, Lung cancer, perfusion CT

1. Introduction

Primary lung cancer is 1 of the most common malignant tumors worldwide, comprising 17% of the total new cancer cases and 23% of total cancer mortality.[1] Early surgery and radio-chemotherapy have been proven to be highly effective in most lung cancer patients. On the contrary, the prognosis of advanced lung cancer patients is still poor, with less than 10% surviving for 5 years.[2] The majority of patients can only be treated by palliation. Generally speaking, early detection and correct diagnosis of lung cancer are important for the treatment, prognosis, and survival of patients with lung cancer.

Contrast-enhanced computed tomography (CT) of the chest remains the most common imaging technique in clinical diagnosis of lung cancer. The characterization of pulmonary nodules revealed by standard contrast-enhanced CT can provide information for differentiating malignancy from benignity.[2] However, since the 1970s, studies have indicated that lung tumors have a dual blood supply of pulmonary circulation and systemic circulation.[3] In the past, due to the limitations of detector width of traditional CT system, and the choice of acquiring time, the pulmonary artery usually could not be included in the perfusion CT imaging territory, in which the input artery was set to the aorta.[4] With the progress of volume scanning technology, the increase of the detector width makes it possible to detect both pulmonary and systemic circulation using dual-input perfusion CT (DI-PCT) technique.[5]

Owing to the greater coverage along the z-axis provided by the 320-row CT system, it is possible to include the pulmonary

Editor: Peng Luo.

This work has received funding from the National Natural Science Foundation of China (81501469) and the Health Industry Special Scientific Research Project of National Health and Family Planning Commission of the People's Republic of China (201402019).

The authors report no conflicts of interest.

Department of Radiology, China-Japan Friendship Hospital, Beijing, China.

* Correspondence: Hongliang Sun, Department of Radiology, China-Japan Friendship Hospital, Beijing 100029, China (e-mail: stentorsun@gmail.com).

Medicine (2017) 96:28(e7479)

Received: 5 April 2017 / Received in final form: 7 June 2017 / Accepted: 18 June 2017

http://dx.doi.org/10.1097/MD.0000000000007479

artery, the aorta, and the tumor in 1 gantry rotation without table movement. DI-PCT, which can acquire more phases than traditional CT, and can simultaneously capture the tumor's first-pass perfusion, makes it possible to assess the dual blood supply in lung tumors with the dual-input maximum slope analysis method. However, there are also significant limitations to DI-PCT. First, in the scanning process, multiple consecutive scans covering the lesion may lead to increased radiation dose.[6–9] Second, the results of postprocessing are affected by many factors, such as the scanning parameters adjustment and mathematical mode.

Dual-energy CT (DE-CT) can provide diagnostic information about the composition of the lesions by using 2 different energy x-rays. By acquiring at 2 different kVp, DE-CT is possible to distinguish different materials, because of different atomic number, energy binding ability, and absorption properties. This technique enables the discrimination of the compositions of specific tissues, such as calculus composition analysis, bone density measurement, and iodine concentration analysis.[10] The main clinical benefit of DE-CT scan as compared with DI-PCT would be that the method is not as susceptible to respiratory motion as the data are acquired within a single breath-hold. Moreover, the radiation dose may be significantly reduced.

Recent studies have shown that DI-PCT and DE-CT iodine maps were significantly correlated.[11] A similar study of the abdomen indicated that the correlation between DE-CT iodine concentration profile and DI-PCT perfusion was significant.[12,13] However, similar studies of lung cancer have not been reported. The objective of this study is to assess the correlation of iodine uptake and perfusion parameters between DE-CT and first-pass DI-PCT in lung cancer patients.

2. Materials and methods

All CT examinations were performed with 320-row multislice spiral CT system (Aquilion ONE, Toshiba Medical Systems, Otawara, Japan). The study, including a pre-experimental and a prospective part, was approved by the ethics committee of our institution. Written informed consent was obtained from all patients before the examination. From March 2015 to October 2016, 45 consecutive patients with suspicious lesions on chest radiography or noncontrast chest CT were enrolled. Inclusion criteria were as follows: without tumor-associated treatment before CT examinations (DI-PCT and DE-CT); the interval between CT examinations (DE-CT and DI-PCT) and CT-guided puncture biopsy or surgical resection was less than 2 weeks; clinical information including pathological results was intact. Also, patients who met any of the following criteria were excluded: hypersensitivity to iodinated contrast media (n = 0); nephropathy (estimated glomerular filtration rate <30 mL/min, n = 0); non-lung cancers (n = 2) confirmed by pathological results. In all, 43 patients with lung lesions were enrolled in the study.

For pre-experimental part of the study: 15 of 43 patients (8 males and 7 females, mean age 64 years, age range 51–78 years) undergoing DE-CT examinations were evaluated to determine the scan time of DE-CT in prospective part of the study.

For prospective part of the study, the remaining 28 patients (19 males and 9 females, mean age 60 years, age range 28–78 years) undergoing DI-PCT and DE-CT examinations were enrolled in the final analysis. The DI-PCT and DE-CT scanning protocols were performed as mentioned below. The DI-PCT and DE-CT can be completed in 1 examination, DE-CT scan was initiated with a delay of 4.5 seconds after DI-PCT.

The radiation dose of the dynamic CT was calculated from the dose-length product (DLP) listed in the exposure summary sheet generated by the CT equipment and multiplied by the correlation coefficient K of 0.014.[14]

2.1. DI-PCT imaging technique

Before the examination, all patients underwent breathing exercise training to ensure that they could hold their breath during the entire perfusion procedure. Superficial and regular abdominal breathing was also permitted in patients who were unable to persist for the entire period of perfusion examination. A 20-gauge intravenous catheter was placed in the antecubital vein to inject the contrast agent.

An initial unenhanced chest CT scan was acquired with a section thickness of 5 mm to localize the tumor and select the volume on which perfusion scans had to be performed. A total of 48 mL of the contrast agent with an iodine concentration of 370 mg I/mL (Iopromide, Bayer Schering, Berlin, Germany) was injected at an injection rate of 6 mL/s. Fifteen consecutive dynamic volume scans with z-axis coverage of 16 cm were performed with a delay of 2 seconds after the start of the injection without table movement.

The dynamic volume scanning parameters were as follows: 100-kv tube voltage, 50-mA tube current, 0.5-second gantry rotation time speed, 0.5-mm slice thickness, 30 seconds total breath-hold time. The first volume scan, acquired before the contrast reaching the heart, served as a baseline, and the other volumes were perfusion scans. After scanning, the scan data were processed with adaptive iterative dose reduction and reconstructed to 320 images per volume with 0.5-mm slice thickness, 0.5-mm slice interval, and a total of 4800 images for the entire perfusion data set.

2.2. Determination of DE-CT initial scanning time

Based on Gordic method of the determination of DE-CT initial scanning time in hepatocellular carcinoma [15] and the enhancement curve of aorta and lung cancer, DE-CT scan is initiated during the peak enhancement of the lung cancer.

The DE-CT acquisition was started along with contrast agent injection, the purpose of which is to obtain at least 1 unenhanced phase for scanning. Each patient was scanned for 11 axial acquisition phases, with 3-second intervals for 1 to 8 phases, 4.5-second intervals for 8 to 9 phases, 5.0-second intervals for 9 to 11 phases, and the total scanning time was 48.7 seconds. The parameters of DE-CT scanning were as follows: gantry rotation, 350 ms; slice thickness, 0.5 mm; single acquisition, 1.2 seconds; tube voltage pair was set at 80 and 135 kVp, both with real-time adjustable variable tube current. Each of the acquisitions covered the same craniocaudal width of 160 mm. Following all the acquisitions, DE-CT images were reconstructed with a section thickness of 0.5 mm and intervals of 0.5 mm for evaluation.

In the postprocessing, to derive the peak enhancement of aorta and the pulmonary artery, the arterial input curve of contrast agent concentration was required by drawing a region of interest (ROI 25 mm^2) the aorta and the pulmonary artery at the level of carina of trachea. The ROI was drawn freehand around the maximum peripheral boundary of the visible tumor on axial imaging. Care was taken to exclude the surrounding lung tissue and normal vascular structures, and also the necrotic tissue in the tumor. Then, the time-density curves (TDCs) of the aorta, pulmonary artery, and the lesion were automatically generated.

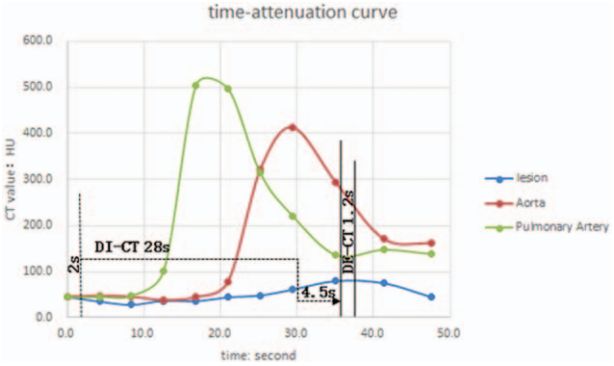

Figure 1. The time-attenuation curves (TDCs) of 1 patient's DE-CT scan shows curves of the lesion (blue), the aortic (red), and the pulmonary artery (green). DI-PCT and DE-CT scan protocols were marked in the diagram. DI-PCT scan was initiated with a delay of 2 seconds after the start of CA injection, and the optimal DE-CT acquisition was set 4.5 seconds after DI-PCT scan.

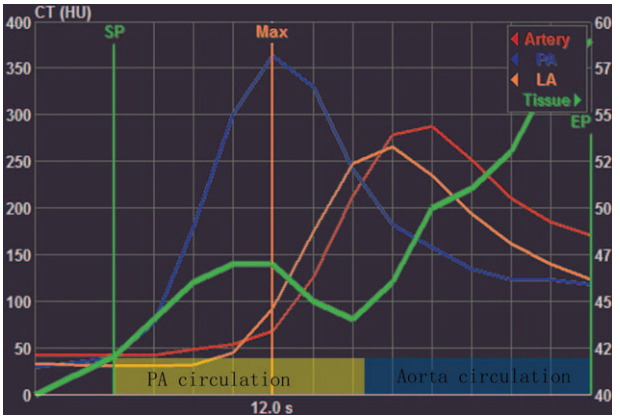

Figure 2. Time-density curves (TDCs) of PF (blue curve), AF (red curve), and left atrium (orange curve) and lung tumor (green, right axis). The vertical orange dotted line indicates the left atrial peak time, which is centered between the PF and AF peaks, representing the boundary between the pulmonary and systemic circulation. During the DI-PCT, 2 peak enhancements were demonstrated from the TDCs of pulmonary circulation and systemic circulation, respectively. The latter one with greater slope demonstrated predominance in this case.

Analysis of the individual and the average time-attenuation indicated that peak enhancement of the aorta was at 28.50 seconds (range 17–38 seconds), pulmonary artery at 19.85 seconds (range 11–27 seconds), and the lesions at 34.5 seconds (range 20–41 seconds). Based on the results above, the optimal DE-CT acquisition was set at the moment of a delay of 34.5 seconds after contrast agent injection, with a duration of 4.5 seconds after DI-PCT scanning (Fig. 1).

2.3. DE-CT imaging technique

The DE-CT scan was initiated with a delay of 34.5 seconds after the start of CA injection. The CT protocol was performed with the following parameters: 0.35-second gantry rotation speed, 0.5-mm slice thickness, 1 acquisition of 1.2 seconds; tube voltage pair was set at 80 and 135 kVp, both with real-time adjustable variable tube current. Each of the acquisitions covered the same craniocaudal width of 160 mm. The scan raw data were reconstructed with a section thickness of 0.5 mm and intervals of 0.5 mm for postprocessing.

2.4. Data postprocessing

The data processing and analysis of the DI-PCT data were performed using perfusion software available on postprocessing system (Body Perfusion, dual-input maximum slope analysis, Toshiba Medical Systems, Otawara, Japan). First of all, volume registration was performed, to correct for motion between the dynamic volumes and create a registered volume series used for subsequent perfusion analysis. After that, circular ROIs (25 mm^2) were manually drawn in the descending aorta, pulmonary artery at the level of carina of trachea, to generate the TDCs representing the bronchial artery flow (BF) input function and pulmonary artery flow (PF) input function. Another circular ROI (25 mm^2) was placed in the left atrium and the time of left atrium TDC was used to differentiate bronchial circulation and pulmonary circulation. Freehand ROIs were delineated along the maximum contours of the visible tumor on axial images, avoiding necrosis and other normal anatomy tissue, then TDC of the contrast medium's first-pass attenuation for lung cancer was automatically generated by the system (Fig. 2). The threshold of perfusion analysis range was set from 0 to 150 HU to restrict the perfusion analysis to soft tissue only and to remove the effects of bone and lung parenchyma. Finally, color-coded maps of AF, PF, and PI were automatically generated by the software with matrix of 512×512. ROIs were placed in the largest solid part of the lesion on axial, sagittal and coronal slices in the maps to measure the AF, PF, and PI values of the whole tumor.

The DE-CT data postprocessing were analyzed using software package available in the Toshiba workstation (DE Raw Data Analysis, Toshiba Medical Systems, Otawara, Japan). After DE-CT data were loaded, the software automatically generated 2×2 groups of images, including 2 single-energy images, a mixed-energy image, and a density-energy curve. A freehand ROI was placed encompassing the solid part of the lesion in the same way with DI-PCT analysis. The CT values (HU) of the lesion were measured in the single energy of 40 KeV image and 70 KeV image, respectively. The difference ($\lambda = 40$ KeV CT value 70 KeV CT value) and the slope ($\lambda HU = \lambda / [40 - 70]$) served as estimates of iodine uptake at the lesion. Finally, a color-coded iodine concentration profile was generated by the software.[16]

2.5. Data statistical analysis

Data analysis was performed using statistical software (SPSS 19.0). The reproducibility of DI-PCT and DE-CT derived parameters between different observers was evaluated with intraclass correlation coefficients (ICCs). ICC values smaller than 0.4 indicate poor reproducibility, those ranging from 0.4 to 0.75 indicate fair reproducibility, and those above 0.75 indicate good reproducibility. A single sample Kolmogorov-Smirnov test was performed on AF, PF, PI, λ, and λHU to determine whether they were normal distribution. Then the Pearson correlation test was performed between data with normal distribution and Spearman correlation test was performed between data not according without normal distribution. *P* values less than .05 were considered to indicate a significant difference.

2.6. IRB statement

The institutional review board approved this study, and informed consent was obtained from all patients enrolled in the study.

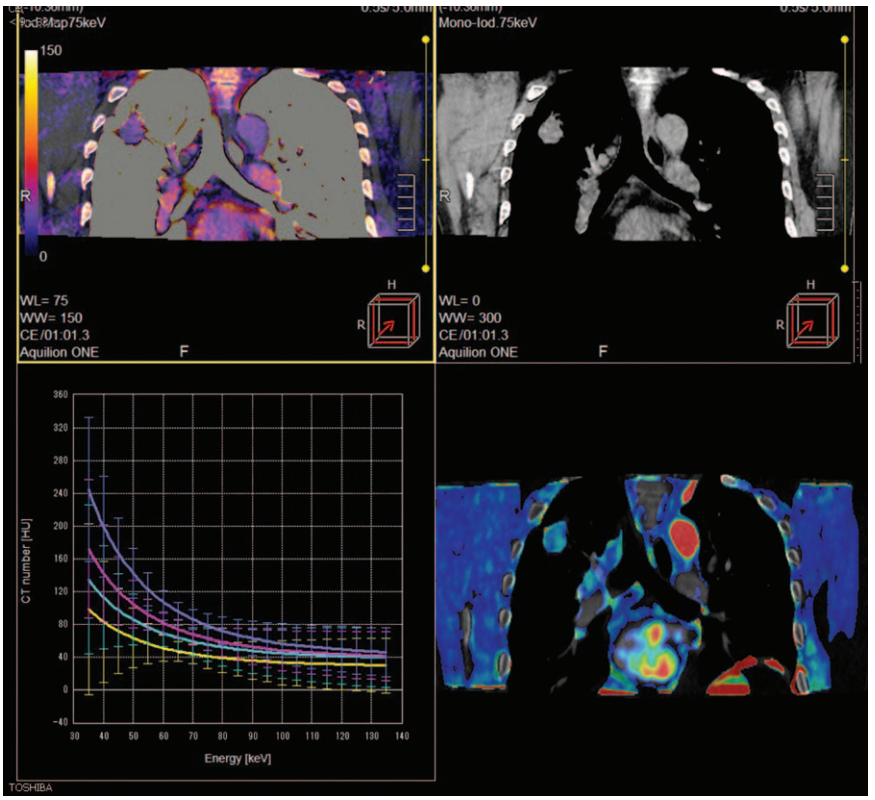

Figure 3. A 63-year-old male patient showed a right upper lobe adenocarcinoma. (A) Iodine map of the lesion showed iodine distribution of the lesion: solid portion with significant iodine uptake. (B) Coronal reconstruction showed the nodule located in the right upper chest. (C) Curves of CT numbers of the aorta (red line), pulmonary artery (dark blue), nodule (light blue), and lymph node (yellow). (D) DE-CT showed the perfusion of the lesion.

3. Results

All subjects were pathologically proved as lung cancers (including 16 squamous cell carcinomas, 8 adenocarcinomas, and 4 small cell lung cancers) by surgery or CT-guided biopsy histology. All the 28 patients successfully completed the examination. No severe adverse events occurred.

Interobserver reproducibility in DI-PCT (PF, AF, PI) and DE-CT (λ, λHU) were relatively good to excellent (ICC_{Inter} = 0.8726–0.9255, ICC_{Inter} = 0.8179–0.8842, ICC_{Inter} = 0.8881–0.9177, ICC_{Inter} = 0.9820–0.9970, ICC_{Inter} = 0.9780–0.9971, respectively).

The DI-PCT perfusion images and the DE-CT iodine profiles are visualized using color-coded maps and matched with the original images (Fig. 3). The measurements of variable parameters are listed in Table 1. The results of correlation coefficient between DI-PCT and DE-CT parameters are demonstrated in Table 2. There was a significant positive correlation between λ and AF, and PF, with a correlation coefficient of 0.589 (P = .001; Fig. 4) and 0.383 (P = .044; Fig. 5). Significant positive correlation was also found between λHU and AF, and PF (r = 0.564, P < .002; r = 0.388, P = .041, respectively) (Figs. 6 and 7). No significant correlation was found between PI and λ, and λHU (P = .346, P = .354, respectively).

The average DLP of DI-PCT was 386.9 mGy·cm, with an effective radiation dose of 5.4 mSv, whereas the average DLP of DE-CT was 193.0 mGy·cm, with a radiation dose of 2.7 mSv.

Table 1

Measurements of parameters derived from different scan modes.

Scan mode	Parameters	Mean ± SD	Range
DI-PCT	AF (mL/min/100 mL)*	61.55 ± 45.05	18.60–379.00
	PF (mL/min/100 mL)	109.40 ± 115.62	13.50–649.40
	PI	58.06 ± 14.13	28.50–82.30
DE-CT	λ (HU)	39.71 ± 21.72	11.20–85.90
	λ (HU)	1.32 ± 0.72	0.40–2.90

λ = the difference of iodine uptake between 40 and 70 KeV in lung lesions, λHU = the slope of iodine uptake between 40 and 70 KeV in lung lesions, AF = aortic flow, DE-CT = dual-energy computed tomography, DI-PCT = dual-input perfusion computed tomography, PF = pulmonary flow, PI = perfusion index, SD = standard deviation.

* AF's value was expressed as median ± interquartile range for its abnormal distribution.

4. Discussion

The results of this study showed good correlations between iodine uptake with DE-CT imaging and perfusion parameters from DI-PCT in lung cancer patients; meanwhile, the exposure dose of DE-CT was significantly lower than that of DI-PCT. In a

Table 2

Results of correlation analysis for parameters between first-pass dual-input perfusion CT and dual-energy CT.

		AF	PF	PI
λ	Correlation coefficient	0.589	0.383	−0.185
	Sig. (2-tailed)	0.001	0.044	0.346
λHU	Correlation coefficient	0.564	0.388	−0.182
	Sig. (2-tailed)	0.002	0.041	0.354

λ = the difference of iodine uptake between 40 and 70 KeV in lung lesions, λHU = the slope of iodine uptake between 40 and 70 KeV in lung lesions, AF = aortic flow, CT = computed tomography, PF = pulmonary flow, PI = perfusion index.

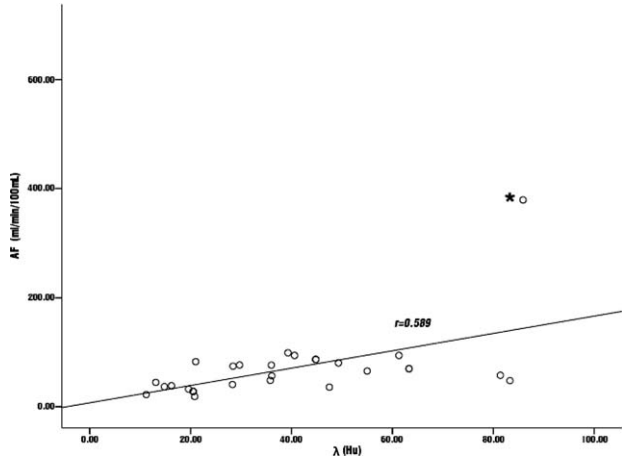

Figure 4. Correlation scatter diagram of AF-λ indicated significant positive correlation, with the correlation coefficient being 0.589 ($P < .01$).

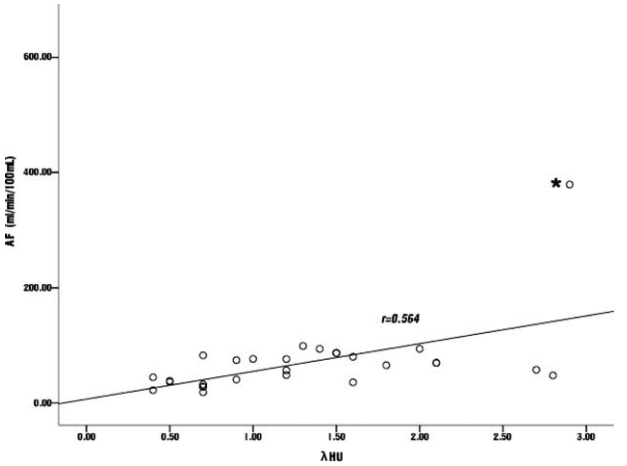

Figure 6. Correlation scatter diagram of AF-slope (λHU) indicated significant positive correlation, with the correlation coefficient being 0.564 ($P < .01$).

rabbit experiment of liver tumors, Zhang et al[11] demonstrated a positive correlation between the iodine maps of the DE-CT acquired during the arterial and the portal venous phases of enhancement and the blood volume determined at perfusion CT. In another study, Fuld et al[17] demonstrated that the pulmonary perfusion blood volume determined at DE-CT could serve as a surrogate for true CT-based measures of the regional pulmonary parenchymal perfusion. By performing DE-CT 15 seconds after contrast agent injection, their study showed good correlation between perfusion CT-based measures of regional pulmonary parenchymal perfusion and DE-CT-based measurements of pulmonary blood volume.

In patients with pancreatic tumors, or liver tumors, or kidney cancer, all the results showed good correlations between parameters acquired from DE-CT and perfusion CT.[7,15,18] In a study of cervical lymph node lesions, Tawfik et al[19] found significant differences in iodine content and iodine overlay acquired from DE-CT between normal, inflammatory lymph nodes, and metastatic squamous cell carcinoma cervical lymph nodes. Moreover, Thaiss et al[20] reported that DE-CT and perfusion CT showed good agreement in terms of diagnosis and evaluation of therapy response. Although multiple studies have shown that there was a good agreement between DE-CT and contrast enhanced or perfusion CT scanning,[21] only a few of studies on the correlation between parameters from DE-CT and DI-PCT in lung cancer patients have been reported.

Traditional contrast-enhanced CT served as the main imaging modality for the diagnosis of lung cancer and has limitations in tumor staging and follow-up. Although the 2 circulations in lung cancer have been found for nearly half a century, the traditional contrast-enhanced CT only demonstrates the dominant circulation. In lung cancer, usually bronchial artery blood supply is more predominant than the pulmonary artery. This feature brings difficulties to differentiate small lesions.[22] With the development of DI-PCT perfusion imaging, tumor hemodynamic parameters derived from perfusion measurements were used to identify lung cancer, which makes CT more suitable for diagnosing, estimating prognosis, and evaluating therapy effect in lung cancer.

Although DI-PCT has many advantages over traditional enhanced CT in qualitative diagnosis, prognosis evaluation, and therapy response evaluation, it still has some limitations. Firstly, DI-PCT requires specialized hardware, with a greater

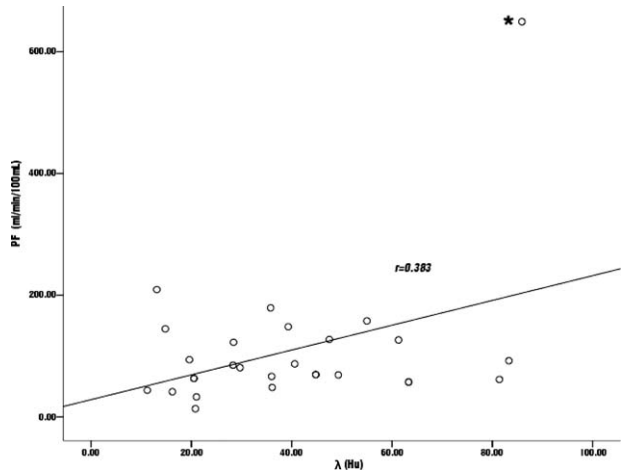

Figure 5. Correlation scatter diagram of PF-λ indicated significant positive correlation, and the correlation coefficient being 0.383 ($P < .05$).

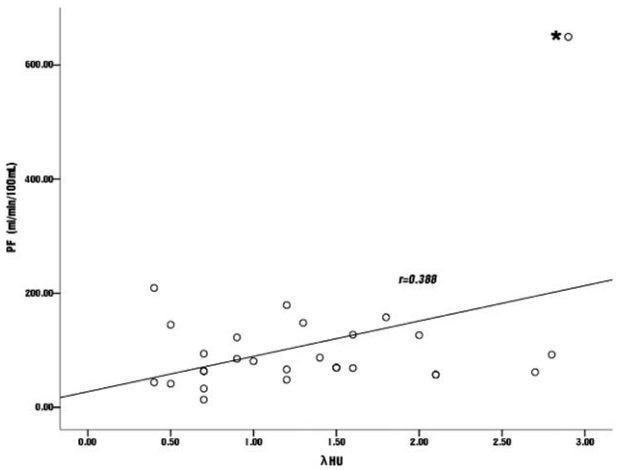

Figure 7. Correlation scatter diagram of PF-slope (λHU) indicated significant positive correlation, with the correlation coefficient being 0.388 ($P < .05$).

width of the detector to cover the entire lesion.[23] Secondly, duration of DI-PCT examination is longer than traditional enhanced CT. In the breath-holding scanning series, patients need to hold breath for a longer time of over 20 seconds, which is difficult for patients with poor respiratory function. Thirdly, DI-PCT requires multiple repeated scans over the same field of view, which significantly increases patients' radiation dose. In addition, there are discrepancies in the different kinetic modeling approaches among vendors and incompatibility between software versions.[24,25]

With the benefit of faster scanning speed and lower exposure dose, DE-CT can reduce scanning time and decrease incidences of radiation adverse events. In addition, analysis of the dual-energy dataset enables the precise iodine enhancement separation and quantification of iodine in a single ROI, owing to the 3-material decomposition algorithm (fat, soft tissue, and iodine). Virtual noncontrast or iodine-enhanced images can also be created.[26] Several previous studies have confirmed the reliability and accuracy of this determination,[27,28] which allows the patient to obtain both noncontrast images and enhanced images in 1 examination, and reduces radiation dose.

The results of our study in lung cancer patients showed that the best mean time point for initiating DE-CT scan was 34.5 seconds after contrast agent injection. In a previous study, the scan of DE-CT was initiated 35 to 40 seconds after injection of contrast agent in scans of the lung with multi-row spiral CT.[29] In studies of pancreatic cancer, DE-CT was initiated about 32 seconds after contrast agent injection, and the parameters obtained from DE-CT have good correlations with those of perfusion CT ($r = 0.77$).[12] The initiating time in our study was similar to those in previous reports, which ensures the accuracy and practicality of parameters analysis. Moreover, during 1 contrast agent injection, patients in our study could take examinations both DI-PCT and DE-CT, which reduced the contrast agent injection. An important issue in DI-PCT is the radiation dose. In our study, the radiation dose of DE-CT was much lower than that of DI-PCT.

The following limitations of this study must be addressed. First, the sample size of patient groups was small and the histopathology of cancer was limited to primary malignancy tumors, which could lead to selection bias. Second, the scanning protocol might not have been ideal, and the scanning time of DE-CT was based on typical cases, which may lead to overestimation of performance. In addition, compared with other studies, more subjects are needed for further trials. For example, whether DI-PCT is reliable in benign and malignant tumors,[30] and in lymph node evaluation, the correlation between DI-PCT, DE-CT, and gold standard FDG-PET/CT is controversial.[31]

5. Conclusions

In conclusion, the correlations of iodine uptake and perfusion parameters in lung cancers between dual-energy CT imaging and first-pass dual-input perfusion CT are significant. Meanwhile, DE-CT needs lower radiation dose and shorter scanning time than DI-PCT. In clinical studies, DE-CT can be used to evaluate the hemodynamic characteristics of lung cancers.

References

[1] Hou WS, Wu HW, Yin Y, et al. Differentiation of lung cancers from inflammatory masses with dual-energy spectral CT imaging. Acad Radiol 2015;22:337–44.

[2] Henzler T, Schmid-Bindert G, Fink C. Pulmonary Nodules and Lung Cancer. Springer, Berlin Heidelberg:2011;101–9.

[3] Milne EN. Circulation of primary and metastatic pulmonary neoplasms: a postmortem microarteriographic study. Am J Roentgenol Radium TheNucl Med 1967;100:603–19.

[4] Yuan X, Zhang J, Quan C, et al. Differentiation of malignant and benign pulmonary nodules with first-pass dual-input perfusion CT. Eur Radiol 2013;23:2469–74.

[5] Yuan X, Zhang J, Ao G, et al. Lung cancer perfusion: can we measure pulmonary and bronchial circulation simultaneously? Eur Radiol 2012;22:1665–71.

[6] Klauss M, Stiller W, Pahn G, et al. Dual-energy perfusion-CT of pancreatic adenocarcinoma. Eur J Radiol 2013;82:208–14.

[7] Klauss M, Stiller W, Fritz F, et al. Computed tomography perfusion analysis of pancreatic carcinoma. J Comput Assist Tomogr 2012;36:237–42.

[8] Kandel S, Kloeters C, Meyer H, et al. Whole-organ perfusion of the pancreas using dynamic volume CT in patients with primary pancreas carcinoma: acquisition technique, post-processing and initial results. Eur Radiol 2009;19:2641–6.

[9] d'Assignies G, Couvelard A, Bahrami S, et al. Pancreatic endocrine tumors: tumor blood flow assessed with perfusion CT reflects angiogenesis and correlates with prognostic factors. Radiology 2009;250:407–16.

[10] Johnson TR, Krauss B, Sedlmair M, et al. Material differentiation by dual energy CT: initial experience. Eur Radiol 2007;17:1510–7.

[11] Zhang LJ, Wu S, Wang M, et al. Quantitative dual energy CT measurements in rabbit VX2 liver tumors: comparison to perfusion CT measurements and histopathological findings. Eur J Radiol 2012;81:1766–75.

[12] Stiller W, Skornitzke S, Fritz F, et al. Correlation of quantitative dual-energy computed tomography iodine maps and abdominal computed tomography perfusion measurements: are single-acquisition dual-energy computed tomography iodine maps more than a reduced-dose surrogate of conventional computed tomography perfusion? Invest Radiol 2015;50:703–8.

[13] Thaiss WM, Haberland U, Kaufmann S, et al. Iodine concentration as a perfusion surrogate marker in oncology: Further elucidation of the underlying mechanisms using Volume Perfusion CT with 80 kVp. Eur Radiol 2016;26:2929–36.

[14] Valentin J. Managing patient dose in multi-detector computed tomography (MDCT). Ann ICRP 2007;37:1–79.

[15] Gordic S, Puippe GD, Krauss B, et al. Correlation between dual-energy and perfusion CT in patients with hepatocellular carcinoma. Radiology 2016;280:78–87.

[16] Liu X, Ouyang D, Li H, et al. Papillary thyroid cancer: dual-energy spectral CT quantitative parameters for preoperative diagnosis of metastasis to the cervical lymph nodes. Radiology 2015;275:167–76.

[17] Fuld MK, Halaweish AF, Haynes SE, et al. Pulmonary perfused blood volume with dual-energy CT as surrogate for pulmonary perfusion assessed with dynamic multidetector CT. Radiology 2013;267:747–56.

[18] Song KD, Kim CK, Park BK, et al. Utility of iodine overlay technique and virtual unenhanced images for the characterization of renal masses by dual-energy CT. AJR Am J Roentgenol 2011;197:1076–82.

[19] Tawfik AM, Razek AA, Kerl JM, et al. Comparison of dual-energy CT-derived iodine content and iodine overlay of normal, inflammatory and metastatic squamous cell carcinoma cervical lymph nodes. Eur Radiol 2014;24:574–80.

[20] Thaiss WM, Sauter AW, Bongers M, et al. Clinical applications for dual energy CT versus dynamic contrast enhanced CT in oncology. Eur J Radiol 2015;84:2368–79.

[21] Chae EJ, Song JW, Seo JB, et al. Clinical utility of dual-energy CT in the evaluation of solitary pulmonary nodules: initial experience. Radiology 2008;249:671–81.

[22] Ohno Y, Koyama H, Matsumoto K, et al. Differentiation of malignant and benign pulmonary nodules with quantitative first-pass 320-detector row perfusion CT versus FDG PET/CT. Radiology 2011;258:599–609.

[23] McCollough CH, Leng S, Yu L, et al. Dual- and multi-energy CT: principles, technical approaches, and clinical applications. Radiology 2015;276:637–53.

[24] Zussman BM, Boghosian G, Gorniak RJ, et al. The relative effect of vendor variability in CT perfusion results: a method comparison study. Am J Roentgenol 2011;197:468–73.

[25] Kudo K, Sasaki M, Yamada K, et al. Differences in CT perfusion maps generated by different commercial software: quantitative analysis by using identical source data of acute stroke patients. Radiology 2010;254:200–9.

[26] Uhrig M, Sedlmair M, Schlemmer HP, et al. Monitoring targeted therapy using dual-energy CT: semi-automatic RECIST plus supplementary functional information by quantifying iodine uptake of melanoma metastases. Cancer Imaging 2013;13:306–13.
[27] Toepker M, Moritz T, Krauss B, et al. Virtual non-contrast in second-generation, dual-energy computed tomography: reliability of attenuation values. Eur J Radiol 2012;81:e398–405.
[28] Phan CM, Yoo AJ, Hirsch JA, et al. Differentiation of hemorrhage from iodinated contrast in different intracranial compartments using dual-energy head CT. AJNR Am J Neuroradiol 2012;33:1088–94.
[29] Bae KT. Intravenous contrast medium administration and scan timing at CT: considerations and approaches. Radiology 2010;256: 32–61.
[30] Harders SW, Madsen HH, Nellemann HM, et al. Dynamic contrast-enhanced CT in suspected lung cancer: quantitative results. Br J Radiol 2013;86:20130257.
[31] Sauter AW, Spira D, Schulze M, et al. Correlation between [18F] FDG PET/CT and volume perfusion CT in primary tumours and mediastinal lymph nodes of non-small-cell lung cancer. Eur J Nucl Med Mol Imaging 2013;40:677–84.